Progress In Electromagnetics Research C, Vol. 21, 59–73, 2011

COMPACT SPATIAL BAND-PASS FILTERS USING FREQUENCY SELECTIVE SURFACES

H. Ghorbaninejad-Foumani and M. Khalaj-Amirhosseini

College of Electrical Engineering
Iran University of Science and Technology, Iran

Abstract—In this paper, spatial-band pass filters consisting of frequency selective surfaces (FSSs) are designed in order to realize both the desired transfer function of the filter in the frequency domain and drastic size reduction. Each FSS is made of aperture elements and patch elements. In this design method, the shape of each FSS is designed by a genetic algorithm (GA) so that the resonant curve of each FSS fits to the resonant curve which can be obtained from an equivalent circuit approach. By locating these designed FSSs at the intervals of quarter wavelength a spatial band pass filter is realized. Furthermore, a technique which controls the frequency response of each FSS has been applied to reduce the longitudinal size of filter. By this technique the FSSs are located at the intervals which are much shorter than a quarter wavelength, keeping the desired transfer function. Through a designed example it is shown that the half longitudinal length of a typical spatial filter can be obtained without any additional structure. Magnetic type spectral domain dyadic Green's functions are derived, and the characteristics of a spatial band-pass filter are calculated by means of the coupled magnetic filed integral equation which accurately takes higher order mode interactions. Derived linear matrix equations are solved using method of moment (MoM). The effectiveness of the proposed structure and its performance are verified and validated by designing and simulating an equal ripple spatial band pass filter at X-band.

Received 4 November 2010, Accepted 28 February 2011, Scheduled 14 April 2011
Corresponding author: Habib Ghorbaninejad Foumani (gh_foumani@yahoo.com).

1. INTRODUCTION

Frequency selective surfaces (FSSs) have significant importance, and they have been investigated in a variety of subjects such as electromagnetic filtering devices for reflector antenna systems, radomes, absorbers, artificial electromagnetic band-gap materials, spatial microwave and optical filters [1–4]. An FSS is a planar structure that is comprised of one or more metallic sheets, each backed by a thin dielectric slab. The overall frequency response of the structure, such as bandwidth, transfer function, and its dependence on the incident wave angle and polarization can be determined by the element type and geometry, substrate parameters and inter element spacing. By now different approaches have been taken to improve FSS performances such as the FSS of antenna-filter-antenna arrays [5], the FSS of aperture coupled micro-strip patches [6], high selectivity waveguide filters by using genetic algorithm designed FSSs [7]. In [8–10], band pass filters based on cascading substrate integrated waveguide (SIW) cavities have been designed.

In this paper, spatial band pass filters using FSSs are designed to realize desired transfer function in frequency domain. Each FSS is made of aperture-type elements and patch-type elements and its shape is obtained using GA to act as a resonator. By locating these designed FSSs at the intervals of quarter wavelength a spatial band pass filter is constructed. Furthermore a technique is used by which the FSSs are located at the intervals which are much shorter than a quarter wavelength, keeping the desired transfer function. To take the effect of higher order modes (evanescent mode), coupled set of magnetic field integral equations are derived which are solved by MoM using sub-domain basis functions. Numerical results obtained from the coupled integral equations technique (CIET) are compared to those from the HFSS [18] software to demonstrate the accuracy of the technique.

2. DESIGN PROCESS OF FSSS

2.1. GA Design

Figure 1 shows the proposed spatial band pass filter consisting of three dielectric backed FSSs. Dielectric backed FSSs work as resonators and quarter wavelength distances $\ell_1 = \ell_2 = \lambda_0/4$ act as invertors in which λ_0 is the free space wavelength. The proposed structure is a two dimensional periodic structure. The FSSs are assumed to be infinitesimally thin and each FSS is backed by a dielectric layer of distinct relative electric permittivity and a given thickness. To design a spatial band pass filter one can calculate an LC prototype resonant

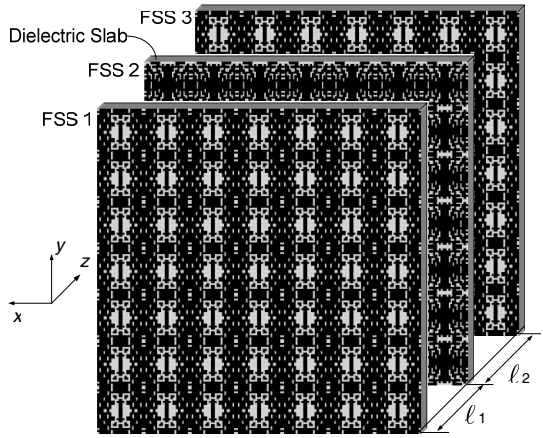

Figure 1. Proposed spatial band pass filter consisting of three FSSs.

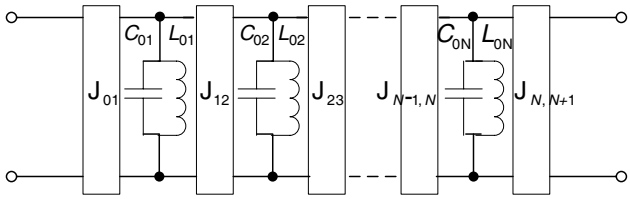

Figure 2. Typical band pass filter using parallel resonators and admittance invertors.

transmission characteristic of each FSS by using the equivalent circuit approach. Fig. 2 shows a band pass filter consisting of N parallel resonators and $N+1$ admittance invertors. The value of admittance invertors and the elements of resonators can be obtained according to the type of filter transfer function, center frequency and the band width of the filter.

Now, we want to model the proposed spatial filter shown in Fig. 1 as a band pass filter shown in Fig. 2. For this purpose after obtaining LC prototype resonant response of each FSS, the shape of FSS can be designed by dividing its unit cell area into $P \times Q$ subsections and using GA [11, 12]. The FSS geometry is represented in terms of 1 s and 0 s in the GA. 1 s and 0 s correspond to the nonmetal and metal parts of FSSs respectively. Here based on the symmetry excitation requirements (incident plane wave) it is assumed that the shape of each FSS in the unit cell is symmetric respect to horizontal and vertical

axes of the unit cell. Consequently GA operates only on one quarter region of unit cell cross section. Now the shape of each resonator can be obtained by GA so that the characteristic of the GA-generated FSS can be fitted on that of an LC prototype resonant curve according to the equivalent circuit model. The fitness function is defined here as

$$\text{fitness} = \sqrt{\frac{\sum_{i=1}^{N_S} \left|S_{21}^{MoM}(f_i) - S_{21}^{LC}(f_i)\right|^2 + \sum_{i=1}^{N_p} \left|S_{21}^{MoM}(f_i) - S_{21}^{LC}(f_i)\right|^2}{N_S + N_P}} \tag{1}$$

where N_S is the number of frequency samples at around resonant point (full transmission point), and N_P is the number of frequency samples at stop band, on the both sides of resonant point. $S_{21}^{MoM}(f_i)$ and $S_{21}^{LC}(f_i)$ are transmission coefficient of each single FSS calculated by moment method and LC equivalent circuit model, both at frequency sample f_i, respectively. After designing each FSS resonator by GA and locating them at the intervals of length $\ell_1 = \ell_2 = \lambda_0/4$, an incident plane wave approximation design is finished. Here the loss of conductors and dielectrics has not been considered for simplicity of design process.

2.2. Coupled Integral Equation Technique Formulation

Consider the unit cell of proposed spatial band pass filter shown in Fig. 3(a) consisting of three dielectric backed FSSs. Relative permittivity of dielectric layers is ε_{r1}, ε_{r2} and ε_{r3} with thickness d_1, d_2 and d_3 respectively. In general, the walls of unit cell are periodic but when this structure excited by an incident plane wave, $\vec{E} = \hat{a}_y E_0 e^{-j\beta z}$ according to the symmetrical conditions, walls which are located at $x = 0$, $x = -d_x$ and $y = 0$, $y = -d_y$ can be replaced by perfect magnetic conducting (PMC) and perfect electric conducting (PEC) respectively. According to equivalence theorem Fig. 3(c) shows the equivalent structure for obtaining fields in varies regions.

Using the conventional spectral domain immitance approach [14, 15] or by any other way one can drive the appropriate magnetic type dyadic Greens function in the spectral domain for these equivalent structures. The enforcement of continuity of transverse magnetic fields across the aperture parts of FSSs at $z = 0$, $z = \ell_1$ and $z = \ell_1 + \ell_2$ in the spatial domain, provides the interaction of all regions [16, 17]. By expressing the magnetic fields in term of their spectral green's functions, then using traditional x- and y-directed piece-wise sinusoidal or roof-top basis and testing functions and applying Galerkin's method one can obtain

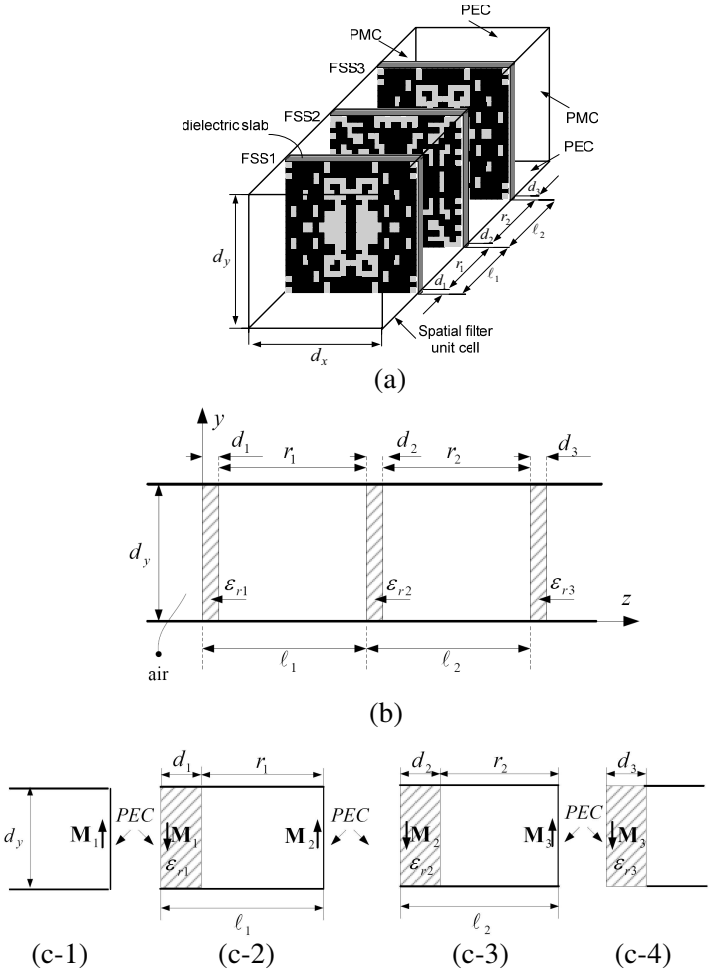

Figure 3. Unit cell of the proposed spatial band pass filter consisting of three FSSs. (a) Three dimensional view. (b) Side view. (c) Equivalent structures for obtaining fields of the proposed structure shown in Fig. 1. (c-1) region $z < 0$, (c-2) region $0 < z < \ell_1$, (c-3) region $\ell_1 < z < \ell_1 + \ell_2$, (c-4) region $z > \ell_2$.

the following matrix equations:

$$\mathbf{A}_1\mathbf{C}_1 + \mathbf{A}_2\mathbf{C}_2 = \mathbf{U} \tag{2}$$

$$\mathbf{A}_3\mathbf{C}_1 + \mathbf{A}_4\mathbf{C}_2 + \mathbf{A}_5\mathbf{C}_3 = \mathbf{0} \tag{3}$$

$$\mathbf{A}_6\mathbf{C}_2 + \mathbf{A}_7\mathbf{C}_3 = \mathbf{0} \tag{4}$$

Each matrix in (2)–(4) is made of (4) or (2) sub matrices. Entries

of these sub matrices are given in the appendix. It is notable that some of these matrices may be equal in symmetrical conditions, a fact which, is used to reduce the computational effort. Also it is worth noting that (2)–(4) follow a clear pattern which allows the number of FSSs to be varied relatively simple.

3. DESIGN EXAMPLE AND RESULTS

In this section, an example of proposed spatial band pass filter is designed and compared with HFSS results. The designed spatial band-pass filter has three FSSs which are located at the intervals of $\ell_1 = \ell_2 = \lambda_0/4 = 7.5\,\text{mm}$. FSSs are supported by small thickness dielectric sheets, $d_1 = d_2 = d_3 = 0.4\,\text{mm}$ and relative electric permittivity of supported dielectric sheets is $\varepsilon_r = 2.5$. A 3-order Chebyshev type spatial band pass filter with center frequency $f_0 = 10\,\text{GHz}$, the relative bandwidth 12 percent and equal ripples 0.2 dB have been designed. The unit cell dimensions $d_x = d_y = 16\,\text{mm}$ is considered. One quarter of each unit cell of the FSS is divided into 12×12 subsections. The GA evaluates S_{21} in frequency range of 9.4–10.6 GHz in pass band as well as 8–9.4 GHz and 10.6–12 GHz in each of the stop bands. The frequency sample points N_P and N_S are set to be 21 in the pass band, and 8 in each of the stop bands at both sides of pass band. GA populations are reproduced through the tournament selection function (tournament size 4), the single-point cross over with the rate P_C of 0.8, and the uniform mutation with the rate P_m of 0.02. The population size is chosen to be 50. Fig. 4 shows the designed FSSs geometries and the comparison between calculated and simulated transmission responses for each FSS. Fig. 5 shows the calculated and simulated transmission responses for designed spatial band pass filter. Fig. 6 shows transmission response of designed filter for some non normal incident plane wave. Comparison between the calculated and simulated results shows good agreement over the frequency range. The length of the filter is 15 mm.

4. SPATIAL FILTERS WITH CLOSELY SPACED FSSS

Based on technique that has been presented in [13], it is straight forward to design spatial filters using closely spaced FSSs. By this method one can design filters whose FSSs intervals are much shorter than a quarter wavelength without any additional structures. In this technique instead of using a quarter wavelength ideal invertors, we use FSS resonators which include a part of ideal FSSs [13]. In these reduced size structures in which FSSs are located closely, the effect of

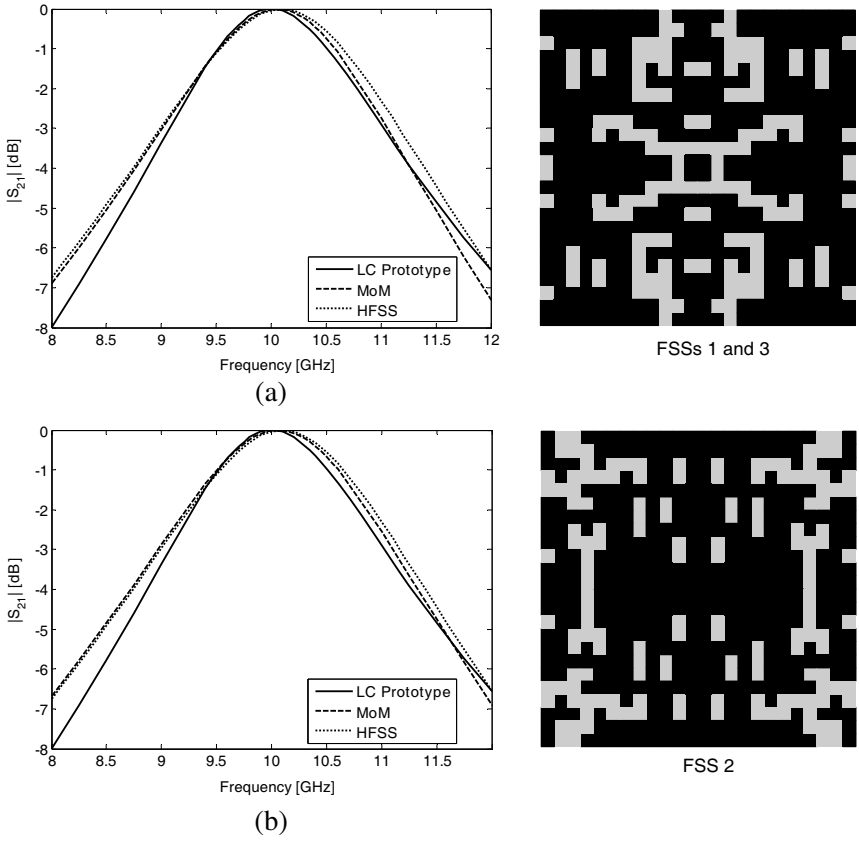

Figure 4. Geometries of designed FSSs and the comparison between calculated and simulated transmission responses for each FSS. (a) FSS1 and FSS3. (b) FSS2.

higher order modes (evanescent mode) between adjacent FSSs must be considered and cannot be neglected. Therefore after designing of each FSS based on resonant-curve fitting separately based on equivalent circuit of closely spaced FSSs [13], we have to repeat optimization by calculating transmission characteristic of whole filter structure and using coupled-integral-equations technique (CIET).

The fitness function is the same as one defined in (1), except that at here $S_{21}^{MoM}(f_i)$ is transmission coefficient of overall filter which is calculated using CIET and MoM and $S_{21}^{LC}(f_i)$ is the transmission coefficient of desired filter which is calculated using prototype LC parameters, both at frequency sample f_i. GA initial population is set the one which have been obtained, based on resonant curve fitting.

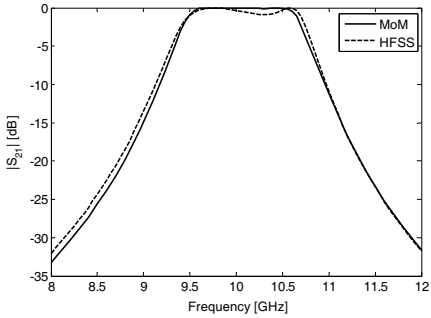

Figure 5. Calculated and simulated transmission response for designed spatial band pass filter.

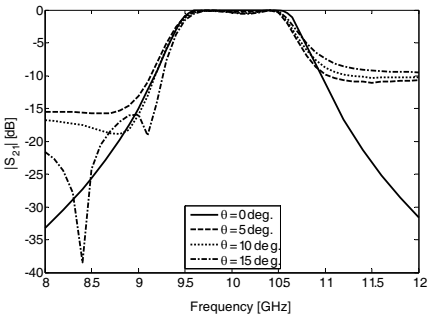

Figure 6. Transmission response for some non normal incident plane wave of Fig. 5.

Since using of CIET is very time consuming though in which Fast Fourier Transform (FFT) is used, in these paper, we have assumed that all of the subsections of FSSs are aperture type initially, and then all of the magnetic currents in frequency samples have been calculated and stored in memory of computer. Finally according to the selected subsections of each FSS, the proper entries can be extracted from general stored matrices. In this approach, transmission and reflected coefficient of each FSS can be calculated from some general matrices which are obtained only once at each frequency sample. When the shape of FSS changes the related coupled integral equations can be extracted from these general matrices in a given frequency and there is not need to repeat all of computation process. By this method, the time needed for GA optimization reduced considerably.

5. REDUCED SIZE SPATIAL FILTER DESIGN EXAMPLE AND RESULTS

In this section, we design a compact spatial Chebyshev bandpass filter, of which the transfer function specification and the dimension of the unit cell are the same as the design example in Section 3. As an example this filter has been designed by three FSSs as resonators, which are supported by small thickness dielectric sheets, $d_1 = d_2 = d_3 = 0.4\,\text{mm}$ and $\ell_1 = \ell_2 = \lambda_0/8 = 3.75\,\text{mm}$, in which λ_0 is the free space wavelength. In this design, the frequency sample points and the GA optimization parameters are the same as the design example in Section 3. Relative electric permittivity of supported dielectric sheets is $\varepsilon_r = 2.5$. Fig. 7 shows the FSSs geometries obtained by the GA and

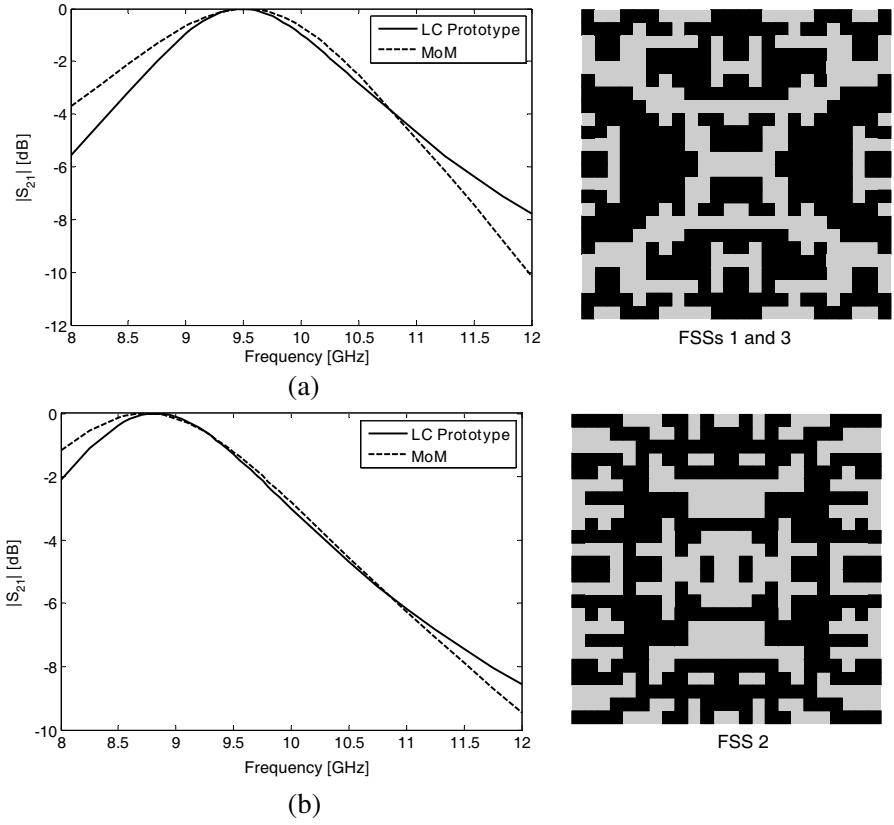

Figure 7. Geometries of designed FSSs and the comparison between calculated and LC prototype transmission responses for each FSS for the reduced size spatial band pass filter. (a) FSS1 and FSS3. (b) FSS2.

transmission characteristic of designed filter and simulated one. The LC prototype transmission characteristic, obtained from equivalent circuit model is also shown in this figure. Although any FSSs do not resonate at the center frequency f_0, the compact spatial filter using this FSSs provide the same transmission characteristic of the design filter with quarter wavelength inverters. Fig. 6 shows the designed FSSs geometries and the comparison between calculated and LC prototype transmission responses for each FSS. Fig. 8 shows Calculated and simulated transmission response for designed reduced-size spatial band pass filter. Fig. 9 shows transmission response of designed filter for some non normal incident plane wave. The longitudinal length of present filter is 7.5 mm, while that of the designed filter with quarter

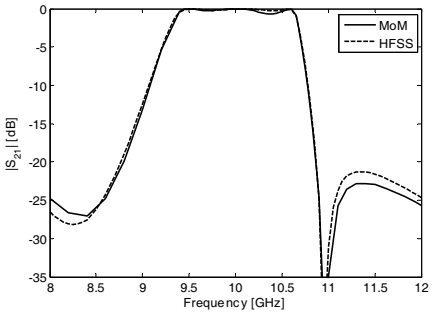

Figure 8. Calculated and simulated transmission response for designed reduced size spatial band pass filter.

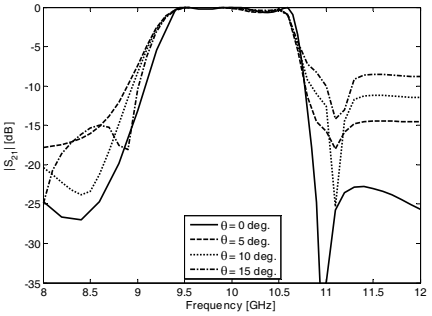

Figure 9. Transmission response for some non normal incident plane wave of Fig. 8.

wavelength inverters is 15 mm. Comparison between the calculated and simulated results shows good agreement over the frequency range.

6. CONCLUSION

In this paper, two spatial band pass filters consisting of FSSs as resonators have been designed. Design process of such filters is basically based on equivalent circuit approach in which FSSs are located in the intervals of quarter wavelength. In this filters each FSS acts as a resonator and quarter wavelength sections act as invertors. The shape of each FSS is designed by a genetic algorithm so that the resonant curve of FSS can be fitted to that obtained from an equivalent circuit approach. In this method it is straight forward to design spatial filters with arbitrarily transfer function. Moreover, using size reduction technique spatial band pass filter, in which the FSSs are closely spaced, has been designed. As an example, a reduced size spatial band pass filter, having the same transmission response as the former design example, has been designed. The total longitudinal length of reduced size spatial bandpass filter becomes about half of the length of non-reduced size filter. It must be noted that in the proposed design method, normal incident wave has been considered. It is apparent that the response of spatial bandpass filter deteriorates as the angle of incidence separates from normal incidence. The numerical and simulated verification shows the usefulness of proposed spatial band pass filter and its design method.

APPENDIX A.

Quantities with a tilde ($\sim$) are Fourier transforms of corresponding quantities without tilde. $\tilde{B}_k^x$ and $\tilde{B}_k^y$ are the Fourier transform of x-directed and y-directed roof top or sinusoidal sub-domain basis functions respectively.

$$\mathbf{A}_i = \begin{bmatrix} \mathbf{A}_{11}^i & \mathbf{A}_{12}^i \\ \mathbf{A}_{21}^i & \mathbf{A}_{22}^i \end{bmatrix}, \quad i = 1, 2, \ldots, 7. \tag{A1}$$

$$\mathbf{C}_i = \begin{bmatrix} \mathbf{C}_{ix} \\ \mathbf{C}_{iy} \end{bmatrix}, \quad i = 1, 2, 3. \tag{A2}$$

$$\mathbf{U} = \begin{bmatrix} \mathbf{U}_{inc,\,x} \\ \mathbf{U}_{inc,\,y} \end{bmatrix} \tag{A3}$$

$$\begin{aligned} \left[\mathbf{A}_{11}^1\right]_{k\ell} &= \sum_{m=0}^{\infty}\sum_{n=0}^{\infty} \tilde{B}_k^x \left(\tilde{G}_{xy}^1 + \tilde{G}_{xy}^2\right) \tilde{B}_\ell^x, \\ \left[\mathbf{A}_{12}^1\right]_{k\ell} &= \sum_{m=0}^{\infty}\sum_{n=0}^{\infty} \tilde{B}_k^x \left(\tilde{G}_{xy}^1 + \tilde{G}_{xy}^2\right) \tilde{B}_\ell^y \\ \left[\mathbf{A}_{21}^1\right]_{k\ell} &= \left[\mathbf{A}_{12}^1\right]_{\ell k}, \\ \left[\mathbf{A}_{22}^1\right]_{k\ell} &= \sum_{m=0}^{\infty}\sum_{n=0}^{\infty} \tilde{B}_k^y \left(\tilde{G}_{xy}^1 + \tilde{G}_{xy}^2\right) \tilde{B}_\ell^y \end{aligned} \tag{A4}$$

$$\begin{aligned} \left[\mathbf{A}_{11}^2\right]_{k\ell} &= \sum_{m=0}^{\infty}\sum_{n=0}^{\infty} \tilde{B}_k^x\, \tilde{G}_{xx}^3\, \tilde{B}_\ell^x, \quad \left[\mathbf{A}_{12}^2\right]_{k\ell} = \sum_{m=0}^{\infty}\sum_{n=0}^{\infty} \tilde{B}_k^x\, \tilde{G}_{xy}^3 \tilde{B}_\ell^y \\ \left[\mathbf{A}_{21}^2\right]_{k\ell} &= \left[\mathbf{A}_{12}^2\right]_{\ell k}, \qquad\qquad \left[\mathbf{A}_{22}^2\right]_{k\ell} = \sum_{m=0}^{\infty}\sum_{n=0}^{\infty} \tilde{B}_k^y\, \tilde{G}_{yy}^3 \tilde{B}_\ell^y \end{aligned} \tag{A5}$$

$$\mathbf{A}_3 = \mathbf{A}_2 \tag{A6}$$

$$\begin{aligned} \left[\mathbf{A}_{11}^4\right]_{k\ell} &= \sum_{m=0}^{\infty}\sum_{n=0}^{\infty} \tilde{B}_k^x \left(\tilde{G}_{xy}^4 + \tilde{G}_{xy}^6\right) \tilde{B}_\ell^x, \\ \left[\mathbf{A}_{12}^4\right]_{k\ell} &= \sum_{m=0}^{\infty}\sum_{n=0}^{\infty} \tilde{B}_k^x \left(\tilde{G}_{xy}^4 + \tilde{G}_{xy}^6\right) \tilde{B}_\ell^y \\ \left[\mathbf{A}_{21}^4\right]_{k\ell} &= \left[\mathbf{A}_{12}^4\right]_{\ell k}, \\ \left[\mathbf{A}_{22}^4\right]_{k\ell} &= \sum_{m=0}^{\infty}\sum_{n=0}^{\infty} \tilde{B}_k^y \left(\tilde{G}_{xy}^4 + \tilde{G}_{xy}^6\right) \tilde{B}_\ell^y \end{aligned} \tag{A7}$$

$$\begin{aligned}
\left[\mathbf{A}_{11}^{5}\right]_{k\ell} &= \sum_{m=0}^{\infty}\sum_{n=0}^{\infty} \tilde{B}_k^x\, \tilde{G}_{xx}^7\, \tilde{B}_\ell^x, \quad \left[\mathbf{A}_{12}^{5}\right]_{k\ell} = \sum_{m=0}^{\infty}\sum_{n=0}^{\infty} \tilde{B}_k^x\, \tilde{G}_{xy}^7 \tilde{B}_\ell^y \\
\left[\mathbf{A}_{21}^{5}\right]_{k\ell} &= \left[\mathbf{A}_{12}^{5}\right]_{\ell k}, \qquad\qquad \left[\mathbf{A}_{22}^{5}\right]_{k\ell} = \sum_{m=0}^{\infty}\sum_{n=0}^{\infty} \tilde{B}_k^y\, \tilde{G}_{yy}^7 \tilde{B}_\ell^y
\end{aligned} \tag{A8}$$

$$\mathbf{A}_6 = \mathbf{A}_5 \tag{A9}$$

$$\begin{aligned}
\left[\mathbf{A}_{11}^{7}\right]_{k\ell} &= \sum_{m=0}^{\infty}\sum_{n=0}^{\infty} \tilde{B}_k^x \left(\tilde{G}_{xy}^8 + \tilde{G}_{xy}^{10}\right) \tilde{B}_\ell^x, \\
\left[\mathbf{A}_{12}^{7}\right]_{k\ell} &= \sum_{m=0}^{\infty}\sum_{n=0}^{\infty} \tilde{B}_k^x \left(\tilde{G}_{xy}^8 + \tilde{G}_{xy}^{10}\right) \tilde{B}_\ell^y \\
\left[\mathbf{A}_{21}^{7}\right]_{k\ell} &= \left[\mathbf{A}_{12}^{7}\right]_{\ell k}, \\
\left[\mathbf{A}_{22}^{7}\right]_{k\ell} &= \sum_{m=0}^{\infty}\sum_{n=0}^{\infty} \tilde{B}_k^y \left(\tilde{G}_{xy}^8 + \tilde{G}_{xy}^{10}\right) \tilde{B}_\ell^y
\end{aligned} \tag{A10}$$

$$\mathbf{C}_{ix} = \begin{bmatrix} C_{i1}^x \\ C_{i2}^x \\ \vdots \\ C_{i,N_{ix}}^x \end{bmatrix}, \quad \mathbf{C}_{iy} = \begin{bmatrix} C_{i1}^y \\ C_{i2}^y \\ \vdots \\ C_{i,N_{iy}}^y \end{bmatrix}, \qquad i = 1\,,\, 2\,,\, 3\,. \tag{A11}$$

$$[\mathbf{U}_{inc,\,x}]_k = 2Y_a^{TE_{00}}(ab)^{0.5}\tilde{B}_k^{1x}, \quad [\mathbf{U}_{inc,\,y}]_k = 0 \tag{A12}$$

where in (A1)–(A10), $\tilde{G}_{ij}$ $(i\,,\ j = x,\ y)$ are the Fourier Transform of dyadic greens functions and defined as

$$\tilde{G}_{xx}^i = Y^{ih}\sin^2\theta + Y^{ie}\cos^2\theta \tag{A13}$$

$$\tilde{G}_{xy}^i = \left(Y^{ih} - Y^{ie}\right)\sin\theta\cos\theta \tag{A14}$$

$$\tilde{G}_{yx}^i = \tilde{G}_{xy}^i \tag{A15}$$

$$\tilde{G}_{yy}^i = Y^{ih}\cos^2\theta + Y^{ie}\sin^2\theta \tag{A16}$$

where

$$Y^{1e,h} = Y_a^{\mathrm{TM,TE}} \tag{A17}$$

$$Y^{2e,h} = Y_{d1}^{\mathrm{TM,TE}} \frac{Y_a^{\mathrm{TM,TE}} + Y_{d1}^{\mathrm{TM,TE}}\tanh(\gamma_{d1}d_1)\tanh(\gamma_a r_1)}{Y_{d1}^{\mathrm{TM,TE}}\tanh(\gamma_a r_1) + Y_a^{\mathrm{TM,TE}}\tanh(\gamma_{d1}d_1)} \tag{A18}$$

$$\begin{aligned}
Y^{3e,h} = Y_a^{\mathrm{TM,TE}} Y_{d1}^{\mathrm{TM,TE}} &\frac{1}{\cosh(\gamma_{d1}d_1)\cosh(\gamma_a r_1)} \\
&\frac{1}{Y_{d1}^{\mathrm{TM,TE}}\tanh(\gamma_a r_1) + Y_a^{\mathrm{TM,TE}}\tanh(\gamma_{d1}d_1)}
\end{aligned} \tag{A19}$$

$$Y^{4e,h} = Y_a^{\mathrm{TM,TE}} \frac{Y_{d1}^{\mathrm{TM,TE}} + Y_a^{\mathrm{TM,TE}} \tanh(\gamma_{d1} d_1) \tanh(\gamma_a r_1)}{Y_a^{\mathrm{TM,TE}} \tanh(\gamma_{d1} d_1) + Y_{d1}^{\mathrm{TM,TE}} \tanh(\gamma_a r_1)} \tag{A20}$$

$$Y^{5e,h} = Y^{3e,h} \tag{A21}$$

$$Y^{6e,h} = Y_{d2}^{\mathrm{TM,TE}} \frac{Y_a^{\mathrm{TM,TE}} + Y_{d2}^{\mathrm{TM,TE}} \tanh(\gamma_{d2} d_2) \tanh(\gamma_a r_2)}{Y_{d2}^{\mathrm{TM,TE}} \tanh(\gamma_a r_2) + Y_a^{\mathrm{TM,TE}} \tanh(\gamma_{d2} d_2)} \tag{A22}$$

$$Y^{7e,h} = Y_a^{\mathrm{TM,TE}} Y_{d2}^{\mathrm{TM,TE}} \frac{1}{\cosh(\gamma_{d2} d_2) \cosh(\gamma_a r_2)} \frac{1}{Y_{d2}^{\mathrm{TM,TE}} \tanh(\gamma_a r_2) + Y_a^{\mathrm{TM,TE}} \tanh(\gamma_{d2} d_2)} \tag{A23}$$

$$Y^{8e,h} = Y_a^{\mathrm{TM,TE}} \frac{Y_{d2}^{\mathrm{TM,TE}} + Y_a^{\mathrm{TM,TE}} \tanh(\gamma_{d2} d_2) \tanh(\gamma_a r_2)}{Y_a^{\mathrm{TM,TE}} \tanh(\gamma_{d2} d_2) + Y_{d2}^{\mathrm{TM,TE}} \tanh(\gamma_a r_2)} \tag{A24}$$

$$Y^{9e,h} = Y^{7e,h} \tag{A25}$$

$$Y^{10e,h} = Y_{d3}^{\mathrm{TM,TE}} \frac{Y_a^{\mathrm{TM,TE}} + Y_{d3}^{\mathrm{TM,TE}} \tanh(\gamma_{d3} d_3)}{Y_{d3}^{\mathrm{TM,TE}} + Y_a^{\mathrm{TM,TE}} \tanh(\gamma_{d3} d_3)} \tag{A26}$$

where

$$Y_{di}^{\mathrm{TE}} = \frac{\gamma_{di}}{j\omega\mu_0}, \quad i = 1\,,\ 2\,,\ 3\,. \tag{A27}$$

$$Y_{di}^{\mathrm{TM}} = \frac{j\omega\varepsilon_0\varepsilon_{ri}}{\gamma_{di}}, \quad i = 1\,,\ 2\,,\ 3\,. \tag{A28}$$

$$Y_a^{\mathrm{TE}} = \frac{\gamma_a}{j\omega\mu_0} \tag{A29}$$

$$Y_a^{\mathrm{TM}} = \frac{j\omega\varepsilon_0}{\gamma_a} \tag{A30}$$

$$\gamma_a = \sqrt{k_x^2 + k_y^2 - \omega^2\mu_0\varepsilon_0} \tag{A31}$$

$$\gamma_{di} = \sqrt{k_x^2 + k_y^2 - \omega^2\mu_0\varepsilon_0\varepsilon_{ri}}\,, \quad i = 1\,,\ 2\,,\ 3\,. \tag{A32}$$

$$\sin\theta = k_x \Big/ \left(k_x^2 + k_y^2\right)^{0.5} \tag{A33}$$

$$\cos\theta = k_y \Big/ \left(k_x^2 + k_y^2\right)^{0.5} \tag{A34}$$

$$Y_a^{\mathrm{TE}_{00}} = Y_a^{\mathrm{TE}}\big|_{m=0,\,n=0} \tag{A35}$$

REFERENCES

1. Munk, B. A., *Frequency Selective Surfaces: Theory and Design*, Wiley, New York, 2000.
2. Kern, D. J. and D. H. Werner, "A genetic algorithm approach to the design of ultra-thin electromagnetic band-gap absorbers," *Microwave Opt. Technol. Lett.*, Vol. 38, No. 1, 61–64, Jul. 2003.
3. Kern, D. J., D. H. Werner, M. J. Wilhelm, and K. H. Church, "Genetically engineered multi-band high impedance frequency selective surfaces," *Microwave Opt. Technol. Lett.*, Vol. 38, No. 5, 400–403, Sep. 2003.
4. Chen, C., "Scattering by a two-dimensional periodic array of ducting plates," *IEEE Tran. Antennas Propagation*, Vol. 18, 660–665, Sep. 1970.
5. Abbaspour, A., K. Sarabandi, and G. M. Rebeiz, "Antenna-filter-an-antenna arrays as a class of band pass frequency selective surfaces," *IEEE Trans. Microw. Theory Tech.*, Vol. 52, No. 8, 1781–1789, Aug. 2004.
6. Pous, R. and D. M. Pozar, "A frequency-selective surface using aperture coupled micro-strip patches," *IEEE Trans. Antennas Propagation*, Vol. 39, No. 12, 1763–1769, Dec. 1991.
7. Ohira, M., H. Deguchi, M. Tsuji, and H. Shigesawa, "Multi band single-layer frequency selective surface designed by combination of genetic algorithm and geometry-refinement technique," *IEEE Trans. Microw. Theory Tech.*, Vol. 52, No. 11, 2925–2931, Nov. 2004.
8. Zhang, Y. L., W. Hong, K. Wu, J. X. Chen, and H. J. Tang, "Novel substrate integrated waveguide cavity filter with defected ground structure," *IEEE Trans. Microw. Theory Tech.*, Vol. 53, No. 4, 1280–1287, Apr. 2005.
9. Hao, Z. C., W. Hong, J. X. Chen, X. P. Chen, and K. Wu, "Compact super wide band pass substrate integrated waveguide filters," *IEEE Trans. Microw. Theory Tech.*, Vol. 53, No. 9, 2968–2977, Sep. 2005.
10. Luo, G. Q., W. Hong, H. J. Tang, and K. Wu, "High performance frequency selective surface using cascading substrate integrated waveguide cavities," *IEEE Microwave and Wireless Components Letters*, Vol. 16, No. 12, Dec. 2006.
11. Yakovlev, A. B., A. I. Khalil, C. W. Hicks, A. Mortazawi, and M. B. Steer, "The generalized scattering matrix of closely spaced strip and slot layers in waveguide," *IEEE Trans. Microw. Theory Tech.*, Vol. 48, No. 1, 126–137, Jan. 2000.

12. Hill, A. and V. K. Tripathi, "An efficient algorithm for the three-dimen-sional analysis of passive microstrip components and discontinuities for microwave and millimeter-wave integrated circuits," *IEEE Trans. Microw. Theory Tech.*, Vol. 39, No. 1, 83–91, Jan. 1991.
13. Ohira, M., H. Deguchi, M. Tsuji, and H. Shigesawa, "Novel waveguide filters with multiple attenuation poles using dual-behavior resonance of frequency-selective surfaces," *IEEE Trans. Microw. Theory Tech.*, Vol. 53, No. 11, 3320–3326, Nov. 2005.
14. Itoh, T., "Spectral domain immitance approach for dispersion characteristics of generalized printed transmission lines," *IEEE Trans. Microw. Theory Tech.*, Vol. 28, No. 11, 733–736, Jul. 1980.
15. Schmidt, L. P. and T. Itoh, "Spectral domain analysis of dominant and higher order modes in fin-lines," *IEEE Trans. Microw. Theory Tech.*, Vol. 28, No. 11, 981–985, Sep. 1980.
16. Chan, C. H., K. T. Ng, and A. B. Kouki, "A mixed spectral-domain approach for dispersion analysis of suspended planar transmission lines with pedestals," *IEEE Trans. Microw. Theory Tech.*, Vol. 37, No. 11, 1716–1723, Sep. 1989.
17. Amari, S., J. Bornemann, and R. Vahldieck, "Fast and accurate analysis of waveguide filters by the coupled integral equations technique" *IEEE Trans. Microw. Theory Tech.*, Vol. 45, No. 9, Sep. 1997.
18. HFSS Release 10.0, Ansoft Corp., 2003.